Available online at www.sciencedirect.com

SCIENCE DIRECT®

ELSEVIER

Journal of Organometallic Chemistry 691 (2006) 3765–3770

Journal of Organo metallic Chemistry

www.elsevier.com/locate/jorganchem

2,6-Di(4-*t*-butylphenyl)phenyl-group 13 organometallic compounds

Brandon Quillian, Yuzhong Wang, Pingrong Wei, Adele Handy, Gregory H. Robinson *

Department of Chemistry, The University of Georgia, Athens, GA 30602-2556, USA

Received 19 April 2006; received in revised form 12 May 2006; accepted 12 May 2006
Available online 20 May 2006

Abstract

Reaction of MX_3 (M = Al, Ga, In; X = Br, Cl) with RLi (R = 2,6-(4-*t*-$BuC_6H_4)_2C_6H_3$) affords $RGaCl_2 \cdot OEt_2$, **1**, $RAlBr_2 \cdot OEt_2$, **2**, R_2GaCl, **3**, and R_3In, **4**. These sterically demanding compounds have been characterized by elemental analyses, ^1H NMR spectroscopy, and single crystal X-ray diffraction. The geometry about the metal centers in **1** and **2** is best described as distorted tetrahedral while the coordination about the gallium atom in **3** is distorted trigonal planar. Compound **4**, with the indium atom in a trigonal planar environment, is noteworthy as the first example of a tris(*m*-terphenyl)group 13 metal compound. The propeller arrangement of the three ligands in compound **4** serves to virtually encapsulate the metallic center.

Keywords: Aluminum; Gallium; Group 13; Indium; Terphenyl ligand

1. Introduction

Sterically demanding ligands have played a prominent role in the development of group 13 organometallic chemistry. In particular, *m*-terphenyl ligands have been extensively utilized to stabilize low-valent, low-coordinate, organometallic group 13 compounds [1–3]. That the structure and bonding of a given compound may be dramatically tuned as a function of ligand steric loading has been a practical method to afford interesting organometallic compounds with intriguing properties. This concept is elegantly illustrated by cyclogallenes, $M_2[GaR]_3$ (M = Na [4], K [5]; R = 2,6-$Mes_2C_6H_3$; Mes = 2,4,6-$Me_3C_6H_2$), metalloaromatic gallium ring systems [1,6]. Another notable example of this concept is the digallyne, $Na_2[RGa{\equiv}GaR]$ (R = 2,6-(2,4,6-*i*-$Pr_3C_6H_2)_2C_6H_3$) [7]. The digallyne and cyclogallenes are typically prepared by alkali metal reduction of the respective $RGaCl_2$ (R = *m*-terphenyl) species. Surprisingly, efforts to evaluate the organometallic group 13 chemistry of less bulky *m*-terphenyl ligands have been limited. Herein, we report the syntheses and molecular structures of $RGaCl_2 \cdot OEt_2$, **1**, $RAlBr_2 \cdot OEt_2$, **2**, R_2GaCl, **3**, and R_3In, **4** (R = 2,6-di(4-*t*-butylphenyl)phenyl, 2,6-(4-*t*-$BuC_6H_4)_2C_6H_3$). The geometry about the metal centers in **1** and **2** is best described as distorted tetrahedral while the coordination about the gallium atom in **3** approaches distorted trigonal planar. Compound **4**, with the indium atom in a trigonal planar environment, is noteworthy as a rare example of a tris-*m*-terphenyl-group 13 metal compound. The propeller arrangement of the three ligands in **4** serves to effectively shield the indium center.

2. Results and discussion

Investigation of the 2,6-di(4-*t*-butylphenyl)phenyl ligand was undertaken in an effort to gain further insight into the significance of substitution at the *ortho* position of the outer phenyl rings, or the lack thereof, when employing sterically encumbered *m*-terphenyl-based ligands [8]. It has been shown that this ligand has the tendency for facile intramolecular C–H bond activation of the *ortho* position of the outer phenyl ring, which may serve as a mechanism to form an *in situ* generated bidentate ligand that provides robust steric protection for the metal center [9]. The

---

* Corresponding author. Tel.: +1 706 542 1853; fax: +1 706 542 9454/1972.
E-mail address: robinson@chem.uga.edu (G.H. Robinson).

0022-328X/$ - see front matter © 2006 Elsevier B.V. All rights reserved.
doi:10.1016/j.jorganchem.2006.05.024

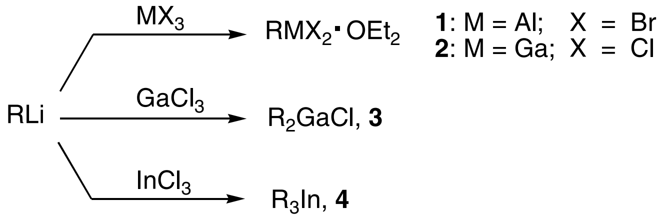

Scheme 1.

literature reveals a paucity of reports of 2,6-di(4-*t*-butylphenyl)phenyl based group 13 compounds [10,11]. The reactivity of RLi (R = 2,6-(4-*t*-$BuC_6H_4)_2C_6H_3$) with group 13 metals was of interest, as to ascertain the stability and structural properties of the ligand–metal complexes. Compounds **1**–**4** were prepared by reaction of the appropriate group 13 halide with RLi (Scheme 1). Although these compounds are all air- and moisture-sensitive, they are stable for months under an inert atmosphere.

Single crystal X-ray analysis reveals that **1** is a monomeric 2,6-di(4-*t*-butylphenyl)phenylgallium chloride etherate with two independent molecules in one asymmetric unit (Fig. 1). Compound **1** is the first single crystal X-ray structurally characterized *m*-terphenylgallium halide etherate, $RGaX_2 \cdot OEt_2$. In general, halide-bridged dimers, $[RGaCl_2]_2$ [12], are usually observed for (*m*-terphenyl)gallium dihalides. Thus, the formation of **1** is notable. Previous structural reports of mono-ligated *m*-terphenylgallium halides are illustrated as neutral monomers without diethyl ether coordination, $RGaCl_2$ [13], dimeric complexes, $[RGaCl_2]_2$ [13–15], and anionic complexes, $[RGaCl_3]^-$ (R = *m*-terphenyl ligand) [16]. Although the synthesis of $RGaCl_2 \cdot OEt_2$ (R = 2,6-(2,4,6-*i*-$Pr_3C_6H_2)_2$-C_6H_3) was previously reported [13], structural data was not presented. The Ga(1)–O(1) distance in **1**, 2.041(4) Å, is only slightly longer than that of (2,4,6-*i*-$Pr_3C_6H_2$)$GaCl_2 \cdot THF$ (2.011(4) Å) [12]. The Ga(1)–O(1) bond distance in **1** is longer than the Ga–O bonds of 2,6-$Mes_2C_6H_3$-based/gallium compounds, R_2GaOH (1.7833(17) Å), $[RGa(Cl)(\mu\text{-}OH)]_2$ (1.938(2)–1.942(2) Å), and $[RGa(Me)(\mu\text{-}OH)]_2$ (1.9110(9)–1.942(2) Å) [17], and exemplifies the weak diethyl ether coordination interaction with the metal in **1**. The C(1)–Ga(1)–O(1) bond angle, 105.89(15)°, is the largest bond angle of those involving the ether donor molecule in **1** and most closely fits with tetrahedral geometry. Notably, the O(1)–Ga(1)–Cl(2) bond angle, 95.05(11)°, is quite small, and although the O(1)–Ga(1)–Cl(1) bond angle, 101.47(11)°, is larger, it still deviates from the expected value. Inspection of the remaining bond angles in **1** reveals that the C(1)–Ga(1)–Cl(1) and C(1)–Ga(1)–Cl(2) bond angles, 123.49(12)° and 118.72(13)°, respectively, are much larger than the Cl(1)–Ga(1)–Cl(2) bond angle, 106.70(6)°, which may be a consequence of steric repulsion between the ligand and chlorides. In fact, acute Cl–Ga–Cl bond angles are common among four coordinate *m*-terphenylgallium chloride complexes. The dimeric complex, $[RGaCl_2]_2$ (R = 2,6-$Mes_2C_6H_3$), was shown to have Cl–Ga–Cl bond angles as small as 86.8(2)° [14,15]. The Ga–C bond distance in **1** of 1.985(5) Å compares well with other *m*-terphenylgallium chloride compounds, which range from 1.930(8) to 1.985(1) Å [13–15,18], and similarly to those in $(Me_5C_6)_3Ga$, (mean bond distance of 1.981(5) Å) [19]. The Ga–Cl bond distances in **1** are unremarkable with a mean bond distance of 2.205 Å.

The structure of **2** (Fig. 2) reveals a four-coordinate aluminum atom in a distorted tetrahedral environment. The

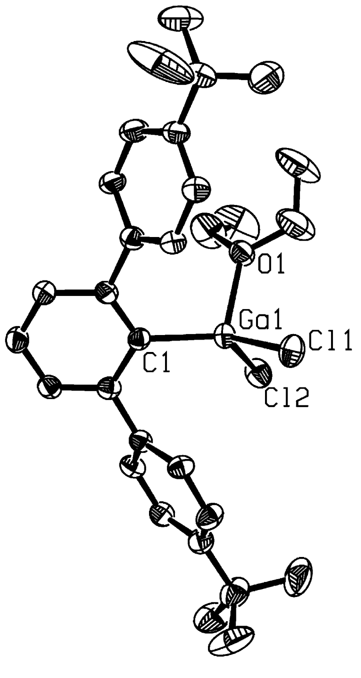

Fig. 1. Molecular structure of (2,6-(4-*t*-$BuC_6H_4)_2C_6H_3$)$GaCl_2 \cdot OEt_2$, **1** (thermal ellipsoids are shown at 35% probability levels). Selected bond distances (Å) and angles (°): Ga(1)–C(1), 1.985(5); Ga(1)–Cl(1), 2.1872(13); Ga(1)–Cl(2), 2.2238(14); Ga(1)–O(1), 2.041(4); C(1)–Ga(1)–Cl(1), 123.49(12); C(1)–Ga(1)–Cl(2), 118.72(13); C(1)–Ga(1)–O(1), 105.89(15); O(1)–Ga(1)–Cl(1), 101.47(11); O(1)–Ga(1)–Cl(2), 95.05(11); Cl(1)–Ga(1)–Cl(2), 106.70(6).

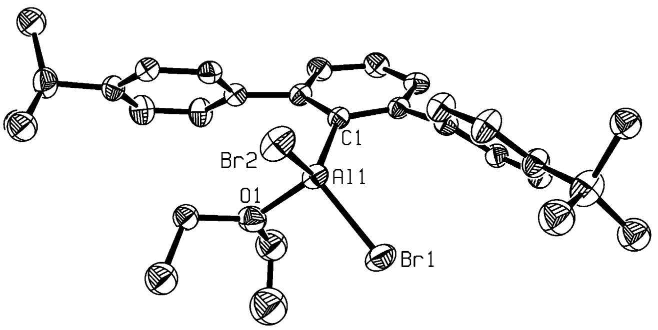

Fig. 2. Molecular structure of (2,6-(4-*t*-$BuC_6H_4)_2C_6H_3$)$AlBr_2 \cdot OEt_2$, **2** (thermal ellipsoids are shown at 35% probability levels). Selected bond distances (Å) and angles (°): Al(1)–C(1), 1.979(5); Al(1)–Br(1), 2.3175(17); Al(1)–Br(2), 2.3010(16); Al(1)–O(1), 1.876(4); C(1)–Al(1)–Br(1), 117.46(15); C(1)–Al(1)–Br(2), 120.10(15); C(1)–Al(1)–O(1), 106.67(19); O(1)–Al(1)–Br(1), 97.94(14); O(1)–Al(1)–Br(2), 104.23(14); Br(1)–Al(1)–Br(2), 107.23(6).

C(1)–Al(1)–Br(1) and C(1)–Al(1)–Br(2) bond angles, 117.46(15)° and 120.10(15)°, respectively, are significantly distorted from classical tetrahedral geometry and are closer to predicted trigonal planar angles. Conversely, the Br(1)–Al(1)–O(1) bond angle, 97.94(14)°, is much smaller than the anticipated 109.5°. An interesting feature of **2** can be seen along the Al–C(1) vector, which is bent away from the phenyl ring plane by 15.54°(avg.). This distortion may be due to packing forces in the crystal lattice, a factor that allows flexibility in the ionic Al–C bond [20]. Comparison of **2** with (2,6-(4-*t*-$BuC_6H_4)_2C_6H_3)AlH_2(NMe_3)$, **5**, is warranted, as it is the only 2,6-di(4-*t*-butylphenyl)phenylaluminum compound [10]. The Al(1)–C(1) bond distance in **2**, 1.979(5) Å, is shorter than that in **5** (2.018(2) Å), but compares well with the *only* other reported *m*-terphenyl stabilized aluminum bromide etherate, $RAlBr_2 \cdot OEt_2$, ($R = 2,4,6\text{-}Ph_3C_6H_2$) (1.983(9) Å) [20], and the organoaluminum bromide dimer, $[RAlBr_3Li]_2$ ($R = 2,6\text{-}Mes_2C_6H_3$), 1.96(2) Å [21]. The structure of **2** shows that the Br(2) atom is almost orthogonal with respect of the central phenyl ring, and the two outer phenyl rings are tilted to it. The Al(1)–Br(1) bond distance in **2**, 2.3175(17) Å, is slightly longer than the Al(1)–Br(2) bond, 2.3010(16) Å, but both are similar to those in $RAlBr_2 \cdot OEt_2$ ($R = 2,4,6\text{-}Ph_3C_6H_2$), (2.297(3) and 2.302(3) Å), but slightly shorter than those in $[RAlBr_3Li]_2$, ($R = 2,6\text{-}Mes_2C_6H_3$), (mean 2.347 Å) [21].

Compound **3** joins a small group of R_2GaX compounds, (R = *m*-terphenyl, X = halide) [14,16,22], although a series of analogous hydrides, alkyls, and a hydroxyl have been reported [17]. The gallium atom in **3** is three-coordinate in a distorted trigonal planar environment (Fig. 3). Correspondingly, other R_2GaX compounds ($R = 2,6\text{-}Ph_2C_6H_3$; X = I [16], and $R = 2,6\text{-}Mes_2C_6H_3$; X = Cl [22], Br [14]), all have distorted trigonal planar environments around the gallium metal center. The C–Ga–Br bond angles in $(2,6\text{-}Mes_2C_6H_3)_2GaBr$, are identical (101.8(2)°). Similarly, the chloride analogue has C–Ga–Cl bond angles of 103.2(4)° and 103.4(4)°. However, the corresponding C(1)–Ga(1)–Cl(1) and C(27)–Ga(1)–Cl(1) bond angles in **3**, 106.69(9)° and 115.76(9)°, respectively, are asymmetric. The C(1)–Ga(1)–C(27) bond angle of **3**, 137.37(12)°, is larger than the C(1)–Ga(1)–C(1a) bond angle (134.3(3)°) in $(2,6\text{-}Ph_2C_6H_3)_2GaI$, but expectedly smaller than that of the "T shaped" $(2,6\text{-}Mes_2C_6H_3)_2GaX$ (X = Cl, Br) compounds (153.5°). The Ga(1)–C(1) and Ga(1)–C(27) bond lengths in **3**, 1.981(3) and 1.997(3) Å, respectively, compare well with other reported diarylgallium halides, while the Ga(1)–Cl(1) bond length in **3**, 2.2537(10) Å, is somewhat longer than that in $(2,6\text{-}Mes_2C_6H_3)_2GaCl$, 2.177(5) Å.

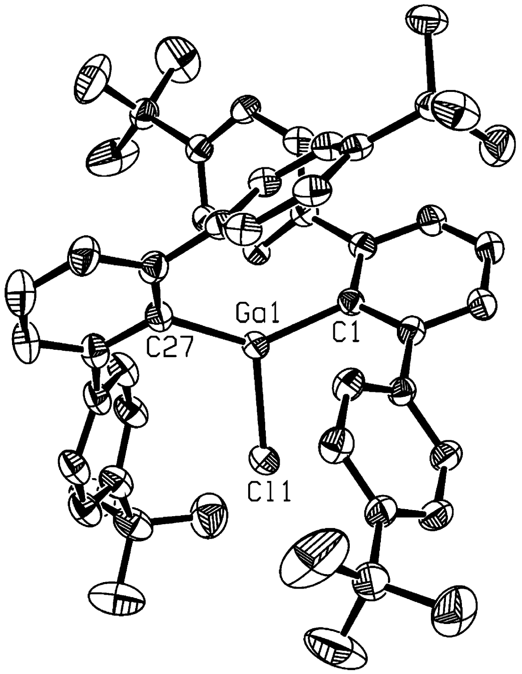

Fig. 3. Molecular structure of (2,6-(4-*t*-$BuC_6H_4)_2C_6H_3)_2GaCl$, **3** (thermal ellipsoids are shown at 35% probability levels). Selected bond distances (Å) and angles (°): Ga(1)–C(1), 1.981(3); Ga(1)–C(27), 1.997(3); Ga(1)–Cl(1), 2.2537(10); C(1)–Ga(1)–C(27), 137.37(12); C(1)–Ga(1)–Cl(1), 106.69(9); C(27)–Ga(1)–Cl(1), 115.76(9).

With the growing utility of triorganoindium compounds for fundamental organic transformations such as conjugate addition [23], cross-coupling [24–26], and allylic substitution reactions [27,28], and the ubiquitous use of *m*-terphenyl ligands in organometallic-group 13 chemistry, it is noteworthy that there are no reports of tris(*m*-terphenyl)indium compounds. Compound **4**, the first tris (*m*-terphenyl)group 13 compound, is noteworthy. The formation of **4** from reaction of RLi and $InCl_3$ in a 1:1 ratio is interesting. The poor solubility of $InCl_3$ may have been a factor in the preparation of **4**. The sharp melting point and accurate elemental analysis is indicative of **4** being the sole product. Consideration of the X-ray structure of **4** provides an interesting contrast from the organo/group 13 halides discussed above (Fig. 4). Compound **4** crystallizes as a monomer with one molecule of diethyl ether per asymmetric unit. The indium atom in **4** is in a distorted trigonal planar coordination environment with C–In–C angles of C(1)–In(1)–C(27), 114.77(13)°; C(1)–In(1)–C(53), 120.34(12)°; C(27)–In(1)–C(53), 124.83(13)° and are similar to those in trimesitylindium, Mes_3In [29], and triphenylindium, Ph_3In [30,31]. However, a twofold axis was observed for Ph_3In that is not evident in **4**. The three ligands in **4** are arranged about the indium atom in a propeller like fashion and are not crystallographically equivalent due to differing dihedral angles with respect to the InC_3-core plane. The dihedral planes were found to be 39.84°, 31.95°, and 65.37° for the C(1), C(27) and C(53) central phenyl ring planes, respectively. The In–C bonds in **4** (In(1)–C(1), 2.200(3) Å; In(1)–C(27), 2.199(3) Å; In(1)–C(53), 2.193(3) Å) are comparable to those in Mes_3In (2.170(5) Å; 2.170(5) Å; 2.163(5) Å), Ph_3In (2.111(14) Å; 2.155(14) Å), and $(2,6\text{-}Mes_2C_6H_3)_2InBr$ (2.171(25) Å; 2.166(26) Å) [32]. These values for **4** are comparable to those in $[(2,6\text{-}Mes_2C_6H_3)InCl_2]_2$ (2.138(8) Å) [33] and $[(2,6\text{-}(2,4,6\text{-}i\text{-}Pr_3C_6H_2)_2C_6H_3)InCl_2]_2$ (2.129(5) Å) [15].

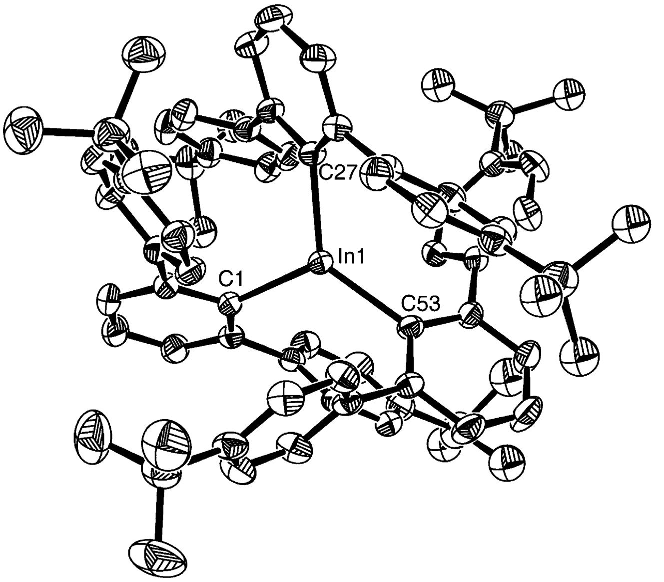

Fig. 4. Molecular structure of (2,6-(4-*t*-BuC_6H_4)$_2$$C_6H_3$)$_3$In, **4** (thermal ellipsoids are shown at 35% probability levels). Selected bond distances (Å) and angles (°): In(1)–C(1), 2.200(3); In(1)–C(27), 2.199(3); In(1)–C(53), 2.193(3); C(1)–In(1)–C(27), 114.77(13); C(1)–In(1)–C(53), 120.34(12); C(27)–In(1)–C(53), 124.83(13).

3. Conclusion

In summary, 2,6-di(4-*t*-butylphenyl)phenyl-based group 13 organometallic compounds, **1**–**4**, have been synthesized and characterized by elemental analyses, ^{1}H NMR spectroscopy, and single crystal X-ray diffraction. Compound **1** represents the first single crystal X-ray structurally characterized *m*-terphenylgallium dihalide etherate, while **4** represents the first reported tris(*m*-terphenyl)group 13 compound.

4. Experimental

4.1. General comments

Standard Schlenk techniques were employed in conjunction with an inert-atmosphere drybox (MBraun Labmaster 130). Solvents were distilled under an argon atmosphere with sodium benzophenone. Argon was passed through copper-based purification and molecular sieve drying columns prior to use. Aluminum(III) bromide, gallium(III) chloride, indium(III) chloride, 4-*tert*-butylphenyl bromide, *n*-butyllithium, and 1,3-dichlorobenzene were purchased from Aldrich Chemical Co. (Milwaukee, WI) and used without further purification. 2,6-Di(4-*tert*-butylphenyl)iodobenzene, 2,6-(4-*t*-BuC_6H_4)$_2$$C_6H_3$I [34], and (2,6-(4-*t*-BuC_6H_4)$_2$$C_6H_3$)Li [35], were prepared according to the literature methods. Elemental analyses were performed by Complete Analysis Laboratories Inc. (Parsippany, NJ). ^{1}H NMR spectra were recorded on a Varian Mercury plus 400 MHz spectrometer.

4.2. Synthesis of (2,6-(4-t-BuC_6H_4)$_2$$C_6H_3$)Ga$Cl_2$ · OEt_2 (1)

GaCl_3 (1.76 g, 10 mmol) in diethyl ether (25 mL) was rapidly transferred to a yellow slurry of (2,6-(4-*t*-BuC_6H_4)$_2$$C_6H_3$)Li (3.47 g, 10 mmol) in diethyl ether (40 mL) at ca. −78 °C and allowed to slowly warm to r.t. After stirring for 48 h, a clear pale yellow solution was filtered from a white precipitate. All solvent was removed *in vacuo* and then the residue was extracted in hexane/diethyl ether (1:1, 20 mL) and placed at r.t. for 2 days, which resulted colorless, cubic crystals (2.13 g, 38% m.p. 212–214 °C), Elemental Anal. Calc. (found) for $C_{30}H_{39}Cl_2GaO$ (556.26): C, 64.78 (64.67); H, 7.07 (6.94); ^{1}H NMR (THF-D_8, 400 MHz) δ 1.116 (q, 6H, –OCH_2C*H*$_3$); 1.360 (s, 18H, C(C*H*$_3$)$_3$); 3.385 (t, 4H, –OC*H*$_2$CH_3); 7.377–7.493 (m, 11H, Ar–H).

4.3. Synthesis of (2,6-(4-t-BuC_6H_4)$_2$$C_6H_3$)Al$Br_2$ · OEt_2 (2)

AlBr_3 (1.29 g, 4.8 mmol) in diethyl ether (30 mL) was rapidly transferred by cannula to a yellow slurry of (2,6-(4-*t*-BuC_6H_4)$_2$$C_6H_3$)Li (1.69 g, 4.8 mmol) in diethyl ether (40 mL) at ca. −78 °C and allowed to warm slowly to r.t. After stirring for 72 h, a colorless solution with white precipitant was observed. The solution was filtered from precipitant and solvent reduced by a third and then placed in freezer at −20 °C. After 3 days a yellow viscous, oily residue formed. The colorless solution was filtered from the oil and then reduced by a third and placed at r.t. for 3 days which gave colorless, rectangular crystals (2.25 g, 78%; m.p. 196–198 °C), Elemental Anal. Calc. (found) for $C_{30}H_{39}AlBr_2O$ (604.42): C, 59.81 (59.64); H, 6.53 (6.50); ^{1}H NMR (D_6-benzene, 400 MHz) δ 0.451 (t, 6H, –OCH_2C*H*$_3$), 1.236 (s, 18H, C(C*H*$_3$)$_3$), 3.219 (q, 4H, –OC*H*$_2$CH_3), 7.347–7.410 (m, 7H, Ar–H), 7.866–7.887 (m, 4H, Ar–H).

4.4. Synthesis of (2,6-(4-t-BuC_6H_4)$_2$$C_6H_3$)$_2$GaCl (3)

GaCl_3 (1.22 g, 6.95 mmol) in diethyl ether (25 mL) was rapidly transferred to a yellow slurry of (2,6-(4-*t*-BuC_6H_4)$_2$$C_6H_3$)Li (4.85 g, 13.9 mmol) in diethyl ether (40 mL) at ca. −78 °C and allowed to slowly warm to r.t. After stirring for 12 h, a clear yellow solution with white precipitant was observed. The solution was filtered from the precipitant and solvent reduced by half. After 3 days at r.t. colorless, cubic crystals formed (2.35 g, 43%; m.p. 202–204 °C), Elemental Anal. Calc. (found) for $C_{52}H_{58}GaCl$ (788.19): C, 79.24 (79.06); H, 7.42 (7.61); ^{1}H NMR (THF-D_8, 400 MHz) δ 1.31 (s, 18H, C(C*H*$_3$)$_3$); 6.987–7.267 (m, 11H, Ar–H).

4.5. Synthesis of (2,6-(4-t-BuC_6H_4)$_2$$C_6H_3$)$_3$In (4)

A yellow slurry of (2,6-(4-*t*-BuC_6H_4)$_2$$C_6H_3$)Li (1.69 g, 4.8 mmol) in diethyl ether (40 mL) was transferred by cannula to a slurry of InCl_3 (1.07 g, 4.8 mmol) in diethyl ether

Table 1
Crystal data and structural refinement for compounds **1**–**4**

Compound	**1**	**2**	**3**	**4**
Empirical formula	$C_{30}H_{39}GaCl_2O$	$C_{60}H_{78}Al_2Br_4O_2$	$C_{52}H_{58}GaCl$	$C_{82}H_{97}InO$
Formula weight	556.23	1204.82	788.15	1213.42
Color, habit	Colorless, cubic	Colorless, cubic	Colorless, cubic	Colorless, cubic
Crystal system	Orthorhombic	Monoclinic	Monoclinic	Triclinic
Space group	$Pna2_1$	$P2_1/n$	$P2_1/n$	$P\bar{1}$
a (Å)	24.640(7)	24.1758(17)	17.587(4)	11.6636(13)
b (Å)	11.365(3)	11.5810(8)	13.911(3)	15.0818(16)
c (Å)	21.545(6)	24.6206(16)	19.968(4)	21.278(2)
α (°)				103.912(2)
β (°)		118.4790(10)	110.010(4)	96.812(2)
γ (°)				90.555(2)
Z	8	4	4	2
V (Å^3)	6033(3)	6059.1(7)	4590.4(16)	3604.6(7)
Maximum 2θ	50	50	50	50
Unique reflections	10,454	10,646	8018	12,638
Observed reflections $[I > 2\sigma(I)]$	8626	6450	5961	10,872
R_1 $[I > 2\sigma(I)]$, wR_2	0.0463, 0.1124	0.0550, 0.1512	0.0472, 0.1284	0.0531, 0.1444
Goodness-of-fit	1.042	1.008	1.019	1.068
Largest difference in peak and hole (e/Å^3)	0.416 and −0.213	0.605 and −0.755	0.789 and −0.188	0.883 and −0.536

(30 mL) at ca. −78 °C. The reaction was allowed slowly warm to r.t. After 3 days of stirring, a clear, colorless solution with an appreciable amount of white precipitant was observed. The solution was filtered from precipitant and solvent reduced and placed in freezer at −20 °C. After 10 days, colorless, flat, rectangular crystals formed (0.21 g, 11.5%; m.p. 288–290 °C), Elemental Anal. Calc. (found) for $C_{78}H_{87}In$ (1139.34): C, 82.23 (82.51); H, 7.70 (7.76); ^1H NMR (D_6-benzene, 400 MHz) δ1.218 (s, 18H, $C(CH_3)_3$), 6.972–7.227 (m, 11H, Ar–H).

4.6. X-ray crystallographic study

Colorless crystals of **1**–**4** were mounted in glass capillaries under an atmosphere of argon in the drybox. The X-ray intensity data were collected at room temperature on a Bruker SMART TM CCD-based X-ray diffractometer system with graphite-monochromated Mo Kα radiation ($\lambda = 0.710–73$ Å), using the ω-scan technique. The structures were solved by direct methods using the SHELXTL 6.1 bundled software package [36]. The data were corrected for Lorentz and polarization effects and integrated with the manufacturer's SAINT software. Absorption corrections were applied with the SADABS. Non-hydrogen atomic scattering factors were taken from the literature tabulations [37]. The heavy atom positions were determined using direct methods employing the SHELXTL routine methods. The remaining non-hydrogen atoms were located from successive difference Fourier map calculations. In the final cycles of each refinement hydrogen atom positions were calculated and allowed to ride on the carbon to which they are bonded assuming a C–H bond length of 0.95 Å. Hydrogen atom temperature factors were fixed at 1.10 times the isotropic temperature factor of the C-atom to which they are bonded. For compound **1**, the non-hydrogen atoms were refined anisotropically except for one carbon atom (C60) on the coordinated ether molecule. For compound **2**, the non-hydrogen atoms were refined anisotropically except for carbon atoms on three disordered ^{t}Bu groups and two disordered ether molecules which coordinate with Al atoms. The three ^{t}Bu groups on the phenyl of the ligand are found disordered in adjacent positions with half occupancies of each, while four ethyl groups on the two diethyl ether groups are found disordered in adjacent positions in four sets which are divided using the PART command. For compound **4** non-hydrogen atoms were refined anisotropically except for four disordered ^{t}Bu groups on the phenyl rings. The four ^{t}Bu groups on the phenyl of ligands are found disordered in adjacent positions with half occupancies of each. Except for the carbon atoms of disordered ^{t}Bu groups, hydrogen atom positions were calculated. Crystallographic data for **1**–**4** are summarized in Table 1.

Acknowledgement

We are grateful to the National Science Foundation and to the donors of the Petroleum Research Fund, administered by the American Chemical Society, for support of this work.

Appendix A. Supplementary material

Crystallographic data (excluding structure factors) for the structures **1**–**4** have been deposited with the Cambridge crystallographic Data Centre **1**: CCDC No. 601863; **2**: CCDC No. 601866; **3** CCDC No. 601864; **4** CCDC No. 601865. These can be obtained free of charge via www.ccdc.cam.ac.uk/data_request/cif, or by emailing data_request@ccdc.cam.ac.uk, or by contacting The Cambridge Crystallographic Data Centre, 12, Union Road, Cambridge CB2 1EZ, UK; fax: +44 1223 336033. Supplementary data associated with this article can be found, in the online version, at doi:10.1016/j.jorganchem.2006.05.024.

References

[1] G.H. Robinson, Acc. Chem. Res. 32 (1999) 773.
[2] G.H. Robinson, Chem. Commun. (2000) 2175.
[3] G.H. Robinson, Adv. Organomet. Chem. 47 (2001) 283.
[4] X.-W. Li, W.T. Pennington, G.H. Robinson, J. Am. Chem. Soc. 117 (1995) 7578.
[5] X.-W. Li, Y. Xie, P.R. Schreiner, K.D. Gripper, R.C. Crittendon, C.F. Campana, H.F. Schaefer, G.H. Robinson, Organometallics 15 (1996) 3798.
[6] Y. Xie, P.R. Schreiner, H.F. Schaefer, X.-W. Li, G.H. Robinson, J. Am. Chem. Soc. 118 (1996) 10635.
[7] J. Su, X.-W. Li, R.C. Crittendon, G.H. Robinson, J. Am. Chem. Soc. 119 (1997) 5471.
[8] R.C. Smith, S. Shah, E. Urnezius, J.D. Protasiewicz, J. Am. Chem. Soc. 125 (2003) 40.
[9] R.J. Wehmschulte, A.A. Diaz, M.A. Khan, Organometallics 22 (2003) 83.
[10] R.J. Wehmschulte, J.J. Ellison, K. Ruhlandt-Senge, P.P. Power, Inorg. Chem. 33 (1994) 6300.
[11] R.J. Wehmschulte, M.A. Khan, B. Twamley, B. Schiemenz, Organometallics 20 (2001) 844.
[12] M.A. Petrie, P.P. Power, H.V. Rasika Dias, K. Ruhlandt-Senge, K.M. Waggoner, R.J. Wehmschulte, Organometallics 12 (1993) 1086.
[13] B.J. Twamley, P.P. Power, Chem. Commun. (1999) 1805.
[14] R.C. Crittendon, X.-W. Li, J. Su, G.H. Robinson, Organometallics 16 (1997) 2443.
[15] J. Su, X.-W. Li, G.H. Robinson, Chem. Commun. (1998) 2015.
[16] R.C. Crittendon, B.C. Beck, J. Su, X.-W. Li, G.H. Robinson, Organometallics 18 (1999) 156.
[17] R.J. Wehmschulte, J.M. Stelle, M.A. Khan, Organometallics 22 (2003) 4678.
[18] B.J. Twamley, P.P. Power, Acta Crystallogr. E57 (2001) m88.
[19] J.K. Vohs, L.E. Downs, M.E. Barfield, S.D. Goodwyn, G.H. Robinson, Polyhedron 21 (2002) 531.
[20] R.J. Wehmschulte, W.J. Grigsby, B. Schiemenz, R.A. Bartlett, P.P. Power, Inorg. Chem. 35 (1996) 6694.
[21] X.-W. Li, J. Su, G.H. Robinson, Chem. Commun. (1998) 1281.
[22] X.-W. Li, W.T. Pennington, G.H. Robinson, Organometallics 14 (1995) 2109.
[23] I. Perez, J.P. Sestelo, M.A. Maestro, A. Mourino, L.A. Sarandeses, J. Org. Chem. 63 (1998) 10074.
[24] S.W. Lee, K. Lee, D. Seomoon, S. Kim, H. Kim, H. Kim, E. Shim, M. Lee, S. Lee, M. Kim, P.H. Lee, J. Org. Chem. 69 (2004) 4852.
[25] I. Perez, J.P. Sestelo, L.A. Sarandeses, J. Am. Chem. Soc. 123 (2001) 4155.
[26] M.A. Pena, J.P. Sestelo, L.A. Sarandeses, Synthesis (2005) 485.
[27] S. Price, S. Edwards, T. Wu, T. Minehan, Tetrahedron Lett. 45 (2004) 5197.
[28] L. Baker, T. Minehan, J. Org. Chem. 69 (2004) 3957.
[29] J.T. Leman, A.R. Barron, Organometallics 8 (1989) 2214.
[30] J.F. Malone, W.S. McDonald, Chem. Commun. (1969) 591.
[31] J.F. Malone, W.S. McDonald, J. Chem. Soc. A (1970) 3362.
[32] X.-W. Li, G.H. Robinson, W.T. Pennington, Main Group Chem. 1 (1996) 301.
[33] G.H. Robinson, X.-W. Li, W.T. Pennington, J. Organomet. Chem. 501 (1995) 399.
[34] A. Saednya, H. Hart, Synthesis (1996) 1455.
[35] N.J. Hardman, B. Twamley, S. Matthias, R. Baldwin, S. Hino, B. Schiemenz, S.M. Kauzlarich, P.P. Power, J. Organomet. Chem. 643–644 (2002) 461.
[36] G.M. Sheldrick, SHELXTL 6.1, Crystallographic Computing System, Siemens Analytical X-ray Instruments, Madison, WI, 2000.
[37] D.T. Cromer, J.T. Waber, International Tables for X-ray Crystallography, Table 2.2B, The Kynoch Press, Birmingham, England, 1974.